MOL #75648

Defining substrate and blocker activity of alanine serine cysteine transporter 2 (ASCT2) ligands with novel serine analogs

Thomas Albers, William Marsiglia, Taniya Thomas, Armanda Gameiro, and Christof Grewer

Department of Chemistry

Binghamton University, Binghamton, NY 13902

Running title: Structure and activity of ASCT2 ligands

Address correspondence to: Christof Grewer, PhD, Department of Chemistry, Binghamton

University, 4400 Vestal Parkway East, Binghamton, NY 13902, Phone: (607) 777-3250, Fax:

(607) 777-4478, E-mail: cgrewer@binghamton.edu

Document Statistics

Number of		
	Text pages:	20
	Tables:	2
	Figures:	8
	References:	37
Number of words in	Abstract:	224
	Introduction:	533
	Discussion:	1500

Abbreviations:

ASCT	alanine-serine-cysteine transporter
DCC	Dicyclohexylcarbodiimide
EAAT	Excicatory amino acid transporter
GlcA$^-$	Gluconate
Glt$_{Ph}$	Glutamate transporter homolog from *Pyrococcus horikoshii*
OMs$^-$	Methanesulfonate
PDB	Protein Data Bank
SLC1	solute carrier 1
RL	Reentrant loop
LAT	System L amino acid transporter

MOL #75648

Abstract

The neutral amino acid transporter ASCT2 belongs to the SLC1 family of solute transporters and transports small, neutral amino acids across the membrane, including the physiologically important and ubiquitous amino acid glutamine. Ou r understanding of t he involvement of ASCT2 in the physiological processes involving glutamine is hampered by a lack of understanding of its pharmacology and the absence of high-affinity inhibitors. In this study, we combined an *in-silico* docking approach with experimental investigation of binding parameters to develop new ASCT2 inhibitors and substrates, a series of serine esters, and to determine structural parameters that govern their functional effects. The series of c ompounds was synthesized using standard methods and exhibited a range of properties, from inhibitors to partial substrates, and full substrates. Our results suggest that amino acid derivatives with small side-chain volume and low side chain hydrophobicity interact strongly with the closed-loop form of the binding site, in which reentrant loop 2, the presumed extracellular gate for the substrate binding site, is closed off. H owever, these derivatives bind weakly to the open-loop form (external gate open to the extracellular side), acting as transported substrates. I n contrast, inhibitors bind preferentially to the open-loop form. An aromatic residue in t he side-chain is required for high-affinity interaction. One of the compounds, the L-serine ester serine biphenyl-4-carboxylate reversibly inhibits ASCT2 function with an apparent affinity of 30 μM.

Introduction

Glutamine is an important amino acid, which is involved in many cellular processes (Neu et al., 1996). Glutamine is shuttled across cellular membranes by a variety of transport systems (Bode, 2001). One of these systems, the neutral amino acid transporter ASCT2, was shown to belong to the solute carrier 1 family of transporters (Utsunomiya-Tate et al., 1996). ASCT2 is specific for transporting small, neutral amino acids, such as glutamine, alanine, serine and cysteine (Bass et al., 1981; Utsunomiya-Tate et al., 1996). In contrast to ASCT2, the closely-related SLC1 family member ASCT1 was shown to lack affinity for glutamine (Arriza et al., 1993). ASCT2 was reported to be an obligate amino acid exchanger (Broer et al., 2000). Thus, amino acid uptake is strictly coupled to amino acid release (exchange) of an intracellular amino acid. This exchange requires the presence of Na^+, since amino acid translocation is coupled to the co-translocation of at least one sodium ion (Broer et al., 2000; Grewer and Grabsch, 2004). In addition to the amino acid exchange function, ASCT2 displays a channel-like anion conductance, which depends on the presence of Na^+ and is amplified by binding of transported substrates and inhibited in the presence of competitive inhibitors (Broer et al., 2000; Grewer and Grabsch, 2004).

ASCT2 is expressed in many tissues, including the brain, in which it may contribute to glutamine homeostasis of neurons and astrocytes (Broer and Brookes, 2001; Deitmer et al., 2003; Gliddon et al., 2009). It was hypothesized, for example, that ASCT2 mediates efflux of glutamine from astrocytes, a process that is critical for the functioning of the glutamate-glutamine cycle, which recycles synaptically-released glutamate. Despite this seemingly important role, the pharmacology of ASCTs is not well understood. While the specificity for a large variety of transported substrates has been studied, not much is known about inhibitors of

ASCT2 amino acid transport (Esslinger et al., 2005; Grewer and Grabsch, 2004). A few inhibitors have been developed based on homology of the amino acid binding site with the related glutamate transporters from the EAAT (excitatory amino acid transporter) family (Grewer and Grabsch, 2004). In particular, a series of glutamine derivatives were developed with substituents that alter the pK_a value of a proposed hydrogen bond donor in form of the amide NH bond (Esslinger et al., 2005). However, affinities were in the 500 µM to low mM range and no distinctions were made with regard to the structural properties that differentiate inhibitors from transported substrates.

Here, we aimed at performing structure function studies in order to develop inhibitors with higher binding affinity, as well as to obtain a better understanding of the molecular determinants of the compounds that differentiate blockers from transported substrates. We have used a docking approach to identify serine derivatives as potential ligands with a series of substituents attached to the hydroxyl oxygen. Experimental validation of the predicted compounds suggests that the activity of the transported substrates decreases strongly after side-chain volume reaches a threshold. In contrast, inhibitors benefit from hydrophobic bulk in the side chain, in particular when the hydrophobic group is aromatic. The analysis resulted in the development of a blocker with approximately 3-fold higher affinity than the best compounds that have been reported previously.

Materials and Methods

Cell culture and transfection. cDNA coding for the rat ASCT2 was kindly provided by S. Bröer (Broer et al., 1999; Broer et al., 2000). The coding region of the cDNA was subcloned into the EcoR*I* site of the pBK-CMV vector (Stratagene). The cDNA construct was used to transiently transfect sub-confluent human embryonic kidney cells (HEK293, ATCC No. CGL

1573) with Fugene HD reagent (Roche Applied Science, Indianapolis), according to the instructions of the supplier. Electrophysiological recordings were performed between days 1 to 2 post-transfection.

Electrophysiological techniques. ASCT2-mediated currents were recorded with an Adams & List EPC7 amplifier (HEKA, Lambrecht, Germany) under voltage-clamp conditions. The whole-cell current-recording configuration was used (Hamill et al., 1981). Electrode resistances were 2-3 MΩ, the series resistance was 5-8 MΩ. Series resistance (R_S), was not compensated, as compensation had no effect on the magnitude of the observed currents. The extracellular bath solution contained (in mM): 140 NaOMs or NaSCN, 2 Mg (GlcA)$_2$, 2 Ca(GlcA)$_2$, and 10 HEPES (pH 7.4 / NaOH). The pipette solution contained (in mM): 130 NaSCN, 2 MgCl$_2$, 10 EGTA, 10 HEPES, and 10 L-alanine (pH 7.3 / NaOH). Using this intracellular solution, the transporters are operated in the exchange mode, in which external alanine is exchanged with internal alanine in the absence of net transport. The exchange mode is associated with the activation of an uncoupled anion current, which was used as an assay for ASCT2 function. The currents were low pass filtered at 3 kHz (EPC7 built-in filter) and digitized with a digitizer board (Digidata 1200, Axon Instruments, Foster City, CA, USA) at a sampling rate of 10-50 kHz (controlled by software, Axon PClamp7). All experiments were performed at room temperature.

Rapid solution exchange was essentially performed as described previously (Grewer et al., 2000; Watzke et al., 2001). Briefly, substrates and inhibitors were applied to the ASCT2-expressing HEK293 cells with a quartz tube (350 μm tube diameter) positioned at a distance of ≈ 0.5 mm to the cell. The linear flow rate of the solutions emerging from the opening of the tube was approximately 5-10 cm/s, resulting in typical rise times of the whole-cell current of 30-50 ms (10 to 90 %).

Data Analysis. Non-linear regression fits of experimental data were performed with Origin (Microcal software, Northampton, MA) or C lampfit (pClamp8 software, Axon Instruments, Foster City, CA). Dose response relationships of currents were fitted with a Michaelis-Menten-like equation, yielding K_m and I_{max}. Each experiment was performed in triplicate with at least two different cells. The error bars represent mean ± S.D., unless stated otherwise.

Docking procedure. H omology models were built using two structures of the Glt$_{Ph}$ as templates, that is PDB refcode 2NWX (aspartate-bound, reentrant loop RL2 closed, (Boudker et al., 2007)) and PDB refcode 2NWW (inhibitor-bound, reentrant loop RL2 open,. Alignments were generated using ClustalW or HHPred (Soding et al., 2005) with similar results, due to the high sequence similarity (85%) in the substrate binding region. O utputs of the pair-wise sequence alignments were used to create structural homology models with the Modeller software (Eswar et al., 2007). For 2NWX as the template, Modeller was programmed to include the two bound cations in the homology model. The resulting structure files were tested for quality with the ProQ program (Wallner and El ofsson, 2003), to test for correct helical assignment of the transmembrane segments.

Docking was performed using the Autodock Vina program (Trott and Olson, 2010), using PyRx as the front-end for li gand preparation and positioning of th e binding box (Wolf, 2009). Ligands were initially generated using ChemSketch (Advanced Chemistry Development, Inc. (ACD/Labs)), setting the correct protonation states for p H 7.3 using Open Babel (http://openbabel.sourceforge.net/). Subsequently, ligands were imported into PyRx and energy-minimized using the UFF force field. The box for docking was set as cubic, 15 Å wide, and centered at the C$_\beta$ atom of the bound amino acid molecule.

Synthesis. All chemicals were purchased from VWR. The compounds were prepared

according to the following procedures:

(S)-3-(*tert*-butoxy)-2-((*tert*-butoxycarbonyl)amino)-3-oxopropyl cyclohexanecarboxylate (1b) In a round-bottom flask, *N*-BOC serine *tert*-butyl ester (0.2g, 0.765mmol) was dissolved in dichloromethane. Cyclohexanecarbonyl chloride (**1a**) was then added along with 4-dimethylaminopyridine (9.3mg, 0.0765mmol) and triethylamine (0.133mL, 0.956mmol). The reaction was stirred overnight. The next day, the mixture was evaporated of dichloromethane, extracted once with cold 2M hydrochloric acid, extracted twice with sodium bicarbonate, and once with brine. The organic layer was dried by passing it through a glass Büchner funnel filled with magnesium sulfate. The material was purified by column chromatography using Ethyl Acetate:Dichloromethane (1:20). ^{1}H NMR (300 MHz, CDCl$_3$) □: 5.3 (s,1H), 4.45 (d, 2H), 2.53 (m, 1H),1.92-1.11 (m, 5H), 1.44 (s, 18H).

(S)-*tert*-butyl-3-(2-(9H-fluoren-3-yl)acetoxy)-2-((*tert*-butoxycarbonyl)amino)propanoate (2b) The serine ester (**2b**) was made using 175mg (0.765mmol) of 9H-fluorene-2-carbonyl chloride (**2a**). Purification of the serine ester was done by column chromatography using the solvent system Dichloromethane:Ethyl Acetate (10:1). ^{1}H NMR (300 MHz, CDCl$_3$) □:8.21 (s, 1H), 8.05 (d, 1H), 7.85 (t, 2H), 7.57 (d, 1H), 7.45 (m, 2H), 4.45 (d, 1H), 4.67-4.51 (m, 3H), 3.95 (s, 2H), 1.51 (s, 18H). **2c**: ^{1}H NMR (300MHz, DMSO-d$_6$) □: 8.95-8.56 (s, 3H), 8.37 (s, 1H), 8.35-8.05 (m, 3H), 7.82-7.65 (m, 1H), 7.64-7.43 (m, 2H), 4.85-4.55 (m, 3H), 4.23-4.07 (s, 2H).

(S)-3-(*tert*-butoxy)-2-((*tert*-butoxycarbonyl)amino)-3-oxopropyl-2-naphthoate (3b) The serine ester (**3b**) was made using 146mg (0.765mmol) of 2-naphthoyl chloride (**3a**). Purification by column chromatography was done using a solvent system of Dichloromethane:Ethyl Acetate (19:1). ^{1}H NMR (300 MHz, CDCl$_3$) □: 8.55 (s, 1H), 8.05-7.81 (m, 4H), 7.55 (m, 2), 5.42 (d, 1H), 4.72-4.56 (m, 3H), 1.45 (s, 18H). **3c:** ^{1}H NMR (300MHz, DMSO-d$_6$) □: 8.91-8.62 (s, 3H),

8.23-8.03 (m, 5H), 7.85-7.71 (m, 2H), 4.89-4.55 (m, 3H).

(S)-*tert*-butyl-2-(*tert*-butoxycarbonyl)amino)-3-(isobutyryloxy)propanoate (4b) The serine ester (4b) was prepared in the same manner, using 67 mg isobutyryl chloride (0.765mmol) (**4a**). The oil was purified using column chromatography using the solvent system Dichloromethane:Ethyl Acetate (1:1). ^{1}H NMR (300 MHz, CDCl$_3$) □: 5.27 (d, 1H), 4.49-4.15 (m, 3H), 2.53 (septet, 1H), 1.45 (s, 18H), 1.16 (d, 6H).

(S)-3-(*tert*-butoxy)-2-((*tert*-butoxycarbonyl)amino)-3-oxopropyl[1,1'-biphenyl]-4-carboxylate (5b) The serine ester was also prepared in the same way as (3b), using 0.17g [1,1'-biphenyl]-4-carbonyl chloride (0.765mmol) (**5a**). The solvent system used for column chromatography was Dichloromethane:Ethyl Acetate (7:3). ^{1}H NMR (300 MHz, CDCl$_3$) □: 8.42-7.40 (m, 9H), 5.51-5.48 (s, 1H), 4.72-4.52 (m, 2H), 3.97-3.83 (m, 1H), 1.68-1.39 (s, 18H).

(S)-*tert*-butyl-2-(*tert*-butoxycarbonyl)amino)-3-(propionyloxy)propanoate (6b) To a solution of propionic acid (51.45mg, 0.695mmol) dissolved in dichloromethane was added *tert*-butyl 2-((*tert*-butoxycarbonyl)amino)-3-hydroxypropanoate (0.2 g, 0. 765 mmol), N,N'-dicyclohexylcarbodiimide (0.16g, 0.765mmol), and 4-dimethylaminopyridine (8.5 mg, 0.0695 mmol). The mixture was magnetically stirred in a rounded bottom flask overnight. The reaction mixture was filtered of N,N'-dicyclohexyl urea and the filtrate was extracted thrice with water, thrice with 5% citric acid in water, and thrice with water. The organic layer was diluted with dichloromethane and was then magnetically stirred overnight in an Erlenmeyer flask with magnesium sulfate to remove traces of water. The organic layer was then filtered and evaporated. The resulting yellow oil was purified using column chromatography. The solvent system used was dichloromethane:ethyl acetate(1:10). ^{1}H NMR (300 MHz, CDCl$_3$) □: 5.28 (d, 1H), 4.45 (d, 2H), 4.25 (m, 1H), 2.34 (q, 2H), 1.45 (s, 18H), 1.11 (t, 3H).

(S)-1-carboxy-2-((cyclohexanecarbonyl)oxy)ethanaminium)tris(2,2,2-trifluoroacetate)

(1c) A mixture of Dichloromethane:Trifluoroacetic acid (1:10) was added to a flask containing **1b**. The mixture was magnetically stirred for three hours and was then evaporated of trifluroacetic acid and dichloromethane to produce the deprotected product **3**. ^{1}H NMR (360MHz, DMSO-d$_6$) □: 8.51 (s, 3H), 4.42 (m, 2H), 4.15 (m,1H), 2.55-1.15 (m, 5H).

The rest of the compounds (2c-6c) were deprotected in the same manner as **1c**. **Mono((S)-2-(((9H-fluorene-2-carbonyl)oxy)-1-carboxyethanaminium)tris(2,2,2-trifluoroacetate) (2c)** ^{1}H NMR (300MHz, DMSO-d$_6$) □: 8.85-8.45 (s,3H), 8.35-7.31 (m, 7H), 4.85-4.47 (m, 3H), 4.23-3.91 (s, 2H) **(S)-2-(((2-naphthoyl)oxy)-1-carboxyethanaminium)tris(2,2,2-trifluoroacetate) (3c)** ^{1}H NMR (300MHz, DMSO-d$_6$) □: 8.83-8.54 (3H), 8.21-7.64 (m, 7H), 4.82-4.51 (m, 3H)**, (S)-1-carboxy-2-((isobutyryloxy)ethanaminium)tris(2,2,2-trifluoroacetate) (4c)** ^{1}H NMR (300MHz, DMSO-d$_6$) □: 8.62-8.43 (s,3H), 4.35 (m, 3H), 2.56 (septet, 1H), 1.12 (s, 6H), **(S)-2-(((([1,1'-biphenyl]-4-carbonyl)oxy)-1-carboxyethanaminium)tris(2,2,2-trifluoroacetate) (5c)** ^{1}H NMR (300MHz, DMSO-d$_6$) □: 8.81-8.62 (s, 3H), 8.21-7.33 (m, 9H), 4.83-4.68 (m, 2H), 4.62-4.50 (m, 1H), **(S)-1-carboxy-2-((propionyloxy)ethanaminium)tris(2,2,2-trifluoroacetate) (6c)** ^{1}H NMR (300MHz, DMSO-d$_6$) □: 8.53-8.45 (s, 3H), 4.63-4.27 (m, 3H), 2.41-2.29 (q, 2H), 1.10-0.99 (t, 3H).

Results

In silico docking studies predict open-loop or closed-loop preference of substrates and inhibitors. In an effort to predict the structure of ligands that interact with the ASCT2 amino acid binding site with reasonable affinity, we used a ligand docking approach. The docking templates were homology models of ASCT2, based on the crystal structures of an homologous archaeal aspartate transporter, Glt$_{Ph}$, (Boudker et al., 2007; Yernool et al., 2004). Although the

overall identity between the ASCT2 and GltPh sequences is low (30% identity, 50% similarity),

the amino acid binding site (residues in 4 Å distance of the bound ligand) is very well conserved

with 69% identity and 85% similarity. In fact, only two side chains that contribute to the ligand

binding site are not conserved, which are C479 (corresponding to R397 in GltPh) and A402

(corresponding to T314 in GltPh). The R-C substitution in TM8 is known to be mainly

responsible for the different substrate selectivities of the two transporters (Bendahan et al.,

2000). In GltPh, the positively-charged side chain of R397 forms a salt bridge with the β-

carboxylate of aspartate (Yernool et al., 2004). This electrostatic interaction is absent in the

ASCTs, accounting for their propensity to bind neutral amino acid substrates.

In order to test the docking approach, we first performed control docking studies using the

known, aspartate-bound crystal structure of Glt_{Ph} as the template (PDB ID 2NWX, (Boudker et

al., 2007)). Docking was performed in Autodock Vina, using a 15 Å cubic box centered at the C_{β}

atom of the bound aspartate molecule. 5 poses were found by the docking algorithm, but only

one of these poses (pose 0 with the lowest binding free energy, table 1) displayed the correct

orientation of the α NH_3^+ and COO^- groups. This pose is shown in Fig. 1A, superimposed with

the native aspartate ligand from the crystal structure (RMSD = 0.73). The slight difference in

predicted and experimental pose is caused by a slightly altered position of the β-carboxylate

(Fig. 1A), whereas the binding positions of the α NH_3^+ and COO^- groups are well preserved.

Overall, this analysis suggests that the docking procedure is capable of detecting physically

relevant conformations of bound ligands in EAAT proteins.

We then used the docking approach to predict the interaction of neutral amino acid derivatives

with ASCT2. We used two separate homology models, based on templates 2NWX, termed

ASCT2(2NWX), and 2NWW, termed ASCT2(2NWW) (Boudker et al., 2007). The former

represents the substrate-bound conformation (closed reentrant loop, RL2, termed *closed-loop* form), whereas the latter was proposed to be more representative of the substrate-free, apo state of the transporter (open RL2, termed *open-loop* form (Boudker et al., 2007; Huang and Tajkhorshid, 2008)). L-Asparagine is a well-characterized transported substrate, which was used first due to its high homology to the aspartate molecule bound to the GltPh template. Only poses with the native orientation of the α NH_3^+ and COO^- groups were evaluated (1 out of 9 for Asn, closed RL2, ASCT2(2NWX), table 1). This pose is shown in Fig. 1B, superimposed over the aspartate molecule bound to the GltPh template, and a docked serine ligand. In contrast to the closed loop conformation, asparagine is predicted to interact less strongly with the open loop configuration (2 out of 5 poses, open RL2, ASCT2(2NWW), table 1), which in GltPh is known to be the inhibitor-bound form (ligand is TBOA, DL-threo-β-Benzyloxyaspartic acid). Similar effects were observed with the native substrates L-glutamine and L-serine (table 1), with glutamine being predicted to bind an order of magnitude more strongly to the closed- than the open-loop form.

In order to test the effect of alterations to the amino acid substrate side chain on docking behavior, we generated serine derivatives with different substituents, linked to the serine hydroxyl with an ester linkage (the structures of the new compounds are illustrated in Fig. 2, together with those of some common amino acid substrates). The ethyl (6c), isopropyl (4c), and cyclohexyl (1c) derivatives could be modeled into the ligand binding site of the closed-loop structure by Autodock Vina. It should be noted that the cyclohexyl (1c) derivative model scored low for binding affinity ($\Delta G = -3.8$ kcal/mol, table 1). Serine derivatives with larger, aromatic substituents (naphtyl (3c) and fluorenyl (2c)), were excluded from the binding site in the closed-loop form (table 1), based on the size of the substituent. In contrast, the naphtyl and fluorenyl

derivative models scored high for binding to the open-loop form, while the compounds with isoproyl substituent and smaller side chains received a low score in this binding configuration (table 1). One of the poses for benzylserine binding to the open-loop form (pose 2 out of 4 poses with correct α NH_3^+ and COO^- group orientation) is shown in Figs. 3A and B, superimposed over the TBOA-bound GltPh structure, 2NWW (Boudker et al., 2007). It is evident that the aromatic group adopts a slightly different orientation in benzylserine compared to TBOA, possibly due to the lack of salt-bridge interaction from the missing β-carboxylate.

As will be discussed in the next paragraphs, our experimental results demonstrate that compounds scoring high for binding to the closed-loop form, but scoring low for binding to the open-loop form are substrates, whereas compounds with the opposite preference for open-loop rather than close-loop binding are inhibitors. To quantify this substrate/inhibitor preference, the ΔG(2NWX model)/ΔG(2NWW model) ratio is listed in table 1 (last column). Compounds with a ratio below 1 are predicted to be inhibitors, whereas compounds with a ratio > 1 are predicted to be substrates.

Experimental analysis of the docking results. Our next aim was to synthesize the compounds predicted from the docking studies and analyze their biological activity. Synthesis was performed according to standard procedures by condensing α NH_2 and COOH-protected serine with the substituent carboxylic acid using either the DCC method (Sheehan et al., 1956), or the acid chloride (Fig. 2), followed by deprotection of the amino acid. The compounds were tested for their ability to either activate anion current, or inhibit leak anion current in ASCT2 heterologously expressed in HEK293 cells. It was previously shown that the transporter-mediated anion current can be used as a measure of transport activity (Broer et al., 2000; Grewer and Grabsch, 2004). This fact is also well established for the homologous glutamate transporters

13

(Watzke and Grewer, 2001), which have a m uch more rigorously determined pharmacology (Bridges and Esslinger, 2005; Bridges et al., 1999; Dunlop and Butera, 2006; Dunlop et al., 2003; Luethi et al., 2010; Shimamoto et al., 1998). Transport current cannot be used as an assay for the function of ASCT2 substrates/inhibitors, because ASCT2 is an amino acid exchanger and, thus, no steady-state transport current can be observed (Broer et al., 2000; Zerangue and Kavanaugh, 1996). However, our results demonstrate that inhibitors block charge movement that is induced by voltage-dependent movement of transported substrates across the membrane (not shown), suggesting that the anion current assay reflects on exchange activity.

Transported substrates are known to induce anion current when applied to ASCT2 (Broer et al., 2000; Grewer and Grabsch, 2004), as shown in F ig. 4A for L-alanine. While acetyl serine ester (6c) was a full substrate, eliciting anion current of the same magnitude as that of alanine, the isobutyryl ester (4c) with the larger substituent volume and increased hydrophobicity was a partial substrate with $26 \pm 10\%$ of the maximal alanine-induced current (at saturating concentration, Fig. 4B, table 2). The kinetic properties of the activating substrates, including their apparent K_m values estimated from dose response curves (Fig. 4B) are listed in table 2. No measurable anion currents were induced by application of serine cyclohexane carboxylate (1c) to ASCT2 (up to 5 mM), indicating that this compound either does not bind to ASCT2 at the tested concentrations, or that it binds, but is not an activating substrate. The former possibility is more likely, as 1c at a concentration up to 2 mM was unable to inhibit alanine-induced inward anion currents mediated by ASCT2 alanine exchange (data not shown).

Next, we tested compounds that were predicted to be inhibitors from the docking studies. In contrast to transported substrates, inhibitor application mediated an apparent outward current in ASCT2-expressing HEK293 cells (representative original traces shown in Fig. 5A). This

outward current was previously shown to be caused by inhibition of a leak inward anion current (Grewer and Grabsch, 2004), in agreement with results obtained for inhibition of the homologous glutamate transporters (EAATs) by the competitive inhibitor TBOA (Grewer et al., 2005; Grewer et al., 2000). The apparent outward current was dose dependent and could be analyzed using a Michaelis-Menten-type equation (Fig. 5B), yielding K_m values listed in table 2. The maximum currents induced by the inhibitors at saturating concentrations (I_{max} values) were -25-30% of those of the maximum alanine-induced current, indicating that the leak anion conductance of ASCT2 carries about 30% of the current of the substrate-induced anion conductance, in agreement with previous results obtained for benzylserine (Grewer and Grabsch, 2004). The inhibitor with the highest apparent affinity was biphenyl serine ester (2c), with a K_m of 30 ± 6 µM. This affinity is significantly higher than any previously known ASCT2 inhibitor (Esslinger et al., 2005; Grewer and Grabsch, 2004).

To test whether the inhibitors not only block leak anion current, but also inhibit activity of transported substrates, we applied the compounds in the presence of alanine (200 µM). As shown in the representative results in Figs. 5C-E, 3c fully inhibited the alanine-induced response and generated leak current block even in the presence of activating substrate (Fig. 5C). Compound 5c was evaluated in more detail, as shown in Figs. 5D, E. The apparent K_I increased with increasing [alanine], as expected for a competitive mechanism. The K_I vs. [alanine] relationship calculated according to eq. 1 (Figure legend 5), fits well to the experimental data, indicating a competitive inhibition mechanism.

Inhibitor dissociation kinetics. We used a rapid solution exchange protocol to determine the dissociation of the naphtyl ester, 3c. The strategy was to pre-equilibrate the cell with the inhibitor, followed by a rapid step into a solution containing a saturating concentration of

alanine (Fig. 6, see bars at the top as an illustration of the solution exchange protocol). If the inhibitor needs to dissociate from the binding site before alanine can bind and elicit anion current, then current activation should be slowed compared to activation by alanine in the absence of the inhibitor. Consistent with this expectation, pre-exposure of ASCT2 to 3c leads to an about two-fold increase in the activation time constant (Fig. 6 A and B). It should be noted that the time resolution of our solution exchange device is in the 5-8 ms range, as tested by recording open pipet tip currents upon changing solutions with varying salt concentrations. Therefore, the activation time constant in the absence of the inhibitor is limited by the time resolution of the solution exchange device. Assuming that the slower kinetics of the inhibitor displacement experiment are not limited by solution exchange kinetics, a dissociation constant of 3c from its binding site of 72 s^{-1} can be estimated.

Structure-activity analysis of ASCT2 substrates and inhibitors. Previous work on the homologous acidic amino acid transporters (EAATs) showed that bulk of the bound amino acid side chain is an important determinant for the strength of interaction of the ligand with its binding site, as well as for defining substrate or inhibitor properties. To test whether ASCT2 ligand behavior obeys similar principles, we analyzed the apparent affinity of the interaction with the protein as a function of amino acid properties, such as side chain volume and hydrophobicity, as defined by log(P) (Fig. 7, P = octanol-water partition coefficient). The data suggest that the affinity of activating substrates increases with decreasing side chain volume, as well as side chain hydrophobicity. In contrast, the affinity of inhibitors increases with increasing side chain volume and log(P) (Fig. 7).

Next, we extended the structure-activity analysis to the ability of the compounds to induce or inhibit anion current. As shown in Fig. 8, compounds with a side chain volume below 110 $Å^3$ are

activating substrates, whereas compounds with higher side chain volume are either inactive (i.e.

do not bind, such as 3c), or inhibit the leak anion conductance. This result suggests the existence

of a size exclusion limit for the binding of activating substrates to their ASCT2 binding site, as

predicted by the docking analysis.

Discussion

Here, we combined in-silico docking with a functional assay to gain insight into the

mechanisms that govern substrate recognition by the neutral amino acid transporter ASCT2. The

docking analysis led to a congeneric series of compounds, which were chemically synthesized

and tested with regard to their ability to activate or inhibit the ASCT2-mediated anion

conductance, a measure for transport activity. The main new result from this study is that

predictors, including side-chain hydrophobicity and volume, allow the classification of

compounds into activating substrates, partial substrates, and inactivating inhibitors. The results

will be useful to more accurately predict ligand behavior in the ASCT2 binding site.

Mechanism of ligand interaction with the binding site. For the related glutamate

transporters, a model for ligand interaction emerges as follows: In the apo, ligand-free state, re-

entrant loop 2 is in an open configuration, allowing low-affinity association of the transported

substrate within the binding cleft. Binding is followed by closure of RL2, resulting in high-

affinity interaction and allowing translocation across the membrane. Transported substrates

presumably bind with higher affinity to the open-loop configuration, because the presence of

RL2 allows for an increased number of hydrogen bonding contacts, as well as hydrophobic

interactions between ligand and protein. Competitive inhibitors, such as TBOA, prevent loop

closure, by positioning the bulky benzyl moiety next to the open RL2, thus preventing

17

translocation. Our docking studies are consistent with this model, suggesting that aspartate preferentially binds to the closed-loop conformation, thus stabilizing it, whereas TBOA preferentially binds to the open-loop configuration. While a c rystal structure of the apo-configuration is not available, MD studies point to the existence of an o pen-loop apo conformation (Huang and Tajkhorshid, 2008).

Our results for ligand binding to the highly-homologous neutral amino acid transporter ASCT2 are consistent with these ideas. In particular, the docking results suggest that compounds that are transported by ASCT2 (activate the anion conductance) bind preferentially to the closed-loop configuration. In contrast, inhibitors are excluded from the closed-loop configuration due to steric clash, but they bind with significant docking scores to the open-loop configuration. Thus, it is likely that ASCT2 inhibitors prevent RL2 closure due to the steric inability of the inhibitor-ASCT2 complex to adopt a closed-loop configuration. Consistent with this model, inhibitor potency, in docking and in the experiment, scales with the volume, as well as the hydrophobicity of the amino acid side chain (Fig. 7). F or transported substrates, our results suggest that they interact poorly with the open loop configuration, but strongly with the closed-loop configuration, thus shifting the equilibrium to the closed-loop form.

It should be noted that for t he inhibitors with the more bulky aromatic substituents, such as fluorenyl and naphtyl, no poses were found, in which the aromatic group associates with the center of RL2. A plausible reason for this behavior is that the side chains are too bulky to fit into the TBOA-homologous open-loop configuration. T his indicates that these inhibitors adopt a different side chain conformation compared to benzylserine or TBOA, which have less aromatic bulk. Alternatively, RL2 may open even further upon substrate dissociation, generating additional room for side-chain interaction. This second alternative is supported by MD

simulation results of GltPh, in which the open-loop conformation on average showed a higher degree of RL2 opening than the TBOA-bound form (Huang and Tajkhorshid, 2008). Therefore, it can be speculated that RL2 can adopt varying degrees of opening, depending on the type of bound substrate, ranging from fully closed for the rapidly-transported substrates, to partially closed for the partial substrates, to fully open for the bulkiest inhibitors. Such a mechanism would not be unprecedented, as in glutamate receptors, which rely on a venus flytrap model for receptor activation by ligand binding (Abele et al., 1999; Armstrong and Gouaux, 2000), the efficacy of the ligand to induce channel opening depends on the degree of domain closure.

Our results suggest that the compound with the naphtyl substituent (3c) dissociates from its binding site with an apparent rate coefficient of $k_d = 72$ s^{-1}. Assuming a dissociation constant of $K_d = 100$ μM, an association rate constant of $k_b = 7 \cdot 10^5$ M^{-1}s^{-1} can be estimated (assuming that $K_d = k_d/k_b$). This rate constant is lower than expected for diffusion-controlled binding. Therefore, it can be hypothesized that binding of bulky inhibitors requires an additional conformational change of the ASCT2 binding site.

Predicting the activating/inhibiting nature of the substrate. One of the main objectives of this study was to be able to develop predictors of ASCT2 substrate behavior. Consistent with results for EAATs, hydrophobic bulk in the side chain aids high affinity interaction with ASCT2, in particular if this bulk is aromatic. Side chain volume can be used to discriminate between transported substrates and inhibitors (Fig. 8), with full substrates exhibiting side chain volumes less than 100 Å^3. Inhibitors have side chain volumes larger than 120 Å^3, with partial substrates somewhere in-between. It is notable that there is a relatively sharp cutoff in side chain volume between substrates and inhibitors.

Interestingly, it is not just hydrophobic bulk in the side chain that is necessary for high-affinity

interaction, but this bulk needs to be aromatic. As is shown in table 2, compound 1c with the cyclohexyl substituent did not interact with ASCT2. This indicates that a large, hydrophobic aliphatic group is not sufficient for bi nding, but that aromatic nature of t he side chain is important. This requirement for aromatic nature is not well represented by the docking results, in which 3c is predicted to bind to the open-loop form with a high docking score (table 2). This is not surprising, as the scoring function only includes a general hydrophobic term in the absence of π-specific interactions (Trott and Olson, 2010). I n the homology model, only two aromatic residues are in the vicinity of th e binding site for potential π-stacking interaction (F391 and W459), but both of these side chains are too far away from the predicted binding location of the aromatic ring(s). Therefore, the detailed physical description of th e binding site interaction awaits further study.

ASCT2 pharmacology. Relatively few inhibitors for amino acid transport by ASCT2 have been developed. In one study, benzylserine was found to be a prototypic competitive ASCT2 inhibitor, based on its structural similarity to the glutamate transporter blocker TBOA (Grewer and Grabsch, 2004). However, benzylserine binds with somewhat low affinity (~1 mM). In another report, a s eries of a sparagine derivatives was investigated, with aromatic groups linked to the amide nitrogen (Esslinger et al., 2005). While no K_i values were given for the compounds, the most potent inhibitor, p-nitrophenyl glutamyl anilide, inhibited 50% of the uptake at about 0.25 mM (Esslinger et al., 2005). Although not knowing the exact K_m value of the C6-cell glutamine transporter for glutamine, it can be estimated that the actual K_i of t he compound is about 80 µM at 100 µM glutamine. Our most potent inhibitor based on th e biphenyl moiety binds with a 30 µM apparent affinity (table 2), suggesting that this represents the highest affinity inhibitor for ASCT2 known to date, surpassing the previous compound in p otency by at least a

20

factor of 3.

Interestingly, the study by Esslinger et al. (Esslinger et al., 2005) concluded that a H-bond donor in the side chain, in form of the amide N-H group, is important for high affinity interaction. However, in our series of compounds no hydrogen bond donor is present at th is position. This result suggests that the H-bond donor is not required for high affinity interaction of inhibitors with the ASCT2 binding site, but it does not exclude the possibility that the introduction of a H -bond donor to the fluorenyl compound could increase affinity. This possibility may be tested in future experiments.

A significant problem for the development of ASCT2 inhibitors is specificity. For example, aryl-asparagine derivatives have been reported as high affinity inhibitors for glu tamate transporters (Greenfield et al., 2005). This indicates that the absence of the negatively-charged β-carboxylate group does not abolish interaction with the binding site of EAATs. Consistently, the ASCT2 inhibitors tested here, except benzylserine, also inhibit the glutamate transporter EAAT3 (data not shown). This is an important finding, as it means that cell biological or neurophysiological studies relying on pharmacological inhibition of glutamate transporters have to be evaluated carefully, since many of the known EAAT inhibitors may also inhibit ASCTs, although their ASCT2 action has never been tested. Therefore, effects may be ascribed to inhibition of EAATs that may partially be caused by inhibition of neutral amino acid transporters. Therefore, it remains a ch allenge to develop high-affinity inhibitors that preferentially bind to ASCTs over EAATs. Pure reliance on hydrophobic bulk in the side chain to achieve high-affinity interaction will not be sufficient to generate selectivity. S pecificity may also be difficult to achieve with respect to other neutral amino acid transporter families. The pharmacology of the System A and System N transporters is not well established, preventing us from commenting on

a possible interaction of our compounds with these transporters. For the System L amino acid transporters, LAT, amino acids with aromatic side chains are substrates (Segawa et al., 1999). Therefore, it is conceivable to assume that aromatic serine esters may also interact with the LAT family of amino acid transporters

Conclusions. In summary, we have used a docking approach, together with experimental validation, to predict substrate and inhibitor behavior of a series of serine derivatives that interact with the binding site of the neutral amino acid transporter ASCT2. Our model predicts that amino acid derivatives with small side-chain volume and low side chain hydrophobicity interact strongly with the closed-loop form of the binding site, but bind weakly to the open-loop form, acting as transported substrates. In contrast, inhibitors bind preferentially to the open-loop form. Side-chain aromaticity is required for high-affinity interaction. These predictions allowed us to develop an inhibitor that binds to ASCT2 with 30 µM apparent affinity, which to our knowledge is currently unsurpassed by other ASCT2 inhibitors. In light of the presumed importance of ASCT2 in glutamine release from proliferating astrocytes, thus potentially contributing to the glutamate-glutamine cycle (Broer and Brookes, 2001), as well as the well known up-regulation of ASCT2 in many cancers (Fuchs and Bode, 2005), the development of new ASCT2 inhibitors may lead to compounds of therapeutic value.

MOL #75648

Authorship contributions

Participated in research design: Albers, Grewer

Conducted experiments: Albers, Marsiglia, Gameiro, Grewer

Contributed new reagents or analytic tools: Albers, Marsiglia, Thomas

Performed data analysis: Albers, Marsiglia, Gameiro, Grewer

Wrote or contributed to the writing of the manuscript: Albers, Marsiglia, Gameiro, Grewer

References

Abele R, Svergun D, Keinanen K, Koch MH and Madden DR (1999) A molecular envelope of the ligand-binding domain of a glutamate receptor in the presence and absence of agonist. *Biochemistry* **38**(34):10949-10957.

Armstrong N and Gouaux E (2000) Mechanisms for activation and antagonism of an AMPA-sensitive glutamate receptor: crystal structures of the GluR2 ligand binding core. *Neuron* **28**(1):165-181.

Arriza J, Kavanaugh M, Fairman W, Wu Y, Murdoch G, North R and Amara S (1993) Cloning and expression of a human neutral amino acid transporter with structural similarity to the glutamate transporter gene family. *J. Biol. Chem.* **268**(21):15329-15332.

Bass R, Hedegaard HB, Dillehay L, Moffett J and Englesberg E (1981) The A, ASC, and L systems for the transport of amino acids in Chinese hamster ovary cells (CHO-K1). *J. Biol. Chem.* **256**(20):10259-10266.

Bendahan A, Armon A, Madani N, Kavanaugh MP and Kanner BI (2000) Arginine 447 Plays a Pivotal Role in Substrate Interactions in a Neuronal Glutamate Transporter. *J. Biol. Chem.* **275**(48):37436-37442.

Bode BP (2001) Recent Molecular Advances in Mammalian Glutamine Transport. *J. Nutr.* **131**(9):2475S-2485.

Boudker O, Ryan RM, Yernool D, Shimamoto K and Gouaux E (2007) Coupling substrate and ion binding to extracellular gate of a sodium-dependent aspartate transporter. *Nature* **445**(7126):387-393.

Bridges RJ and Esslinger CS (2005) The excitatory amino acid transporters: pharmacological insights on substrate and inhibitor specificity of the EAAT subtypes. *Pharmacol. Ther.*

107(3):271-285.

Bridges RJ, Kavanaugh MP and Chamberlin AR (1999) A pharmacological review of competitive inhibitors and substrates of high-affinity, sodium-dependent glutamate transport in the central nervous system. *Curr. Pharm. Des.* **5**(5):363-379.

Broer A, Brookes N, Ganapathy V, Dimmer KS, Wagner CA, Lang F and Broer S (1999) The astroglial ASCT2 amino acid transporter as a m ediator of glu tamine efflux. *J. Neurochem.* **73**(5):2184-2194.

Broer A, Wagner C, Lang F and Broer S (2000) Neutral amino acid transporter ASCT2 displays substrate-induced Na+ exchange and a substrate-gated anion conductance. *Biochem. J.* **346**:705–710.

Broer S and Brookes N (2001) Transfer of glutamine between astrocytes and neurons. *J. Neurochem.* **77**(3):705-719.

Deitmer JW, Broer A and Br oer S (2003) Glutamine efflux from astrocytes is mediated by multiple pathways. *J. Neurochem.* **87**(1):127-135.

Dunlop J and Butera JA (2006) Ligands targeting the excitatory amino acid transporters (EAATs). *Curr. Top. Med. Chem.* **6**(17):1897-1906.

Dunlop J, Eliasof S, Stack G, McIlvain HB, Greenfield A, Kowal D, Petroski R and Ca rrick T (2003) WAY-855 (3-amino-tricyclo[2.2.1.02.6]heptane-1,3-dicarboxylic acid): a novel, EAAT2-preferring, nonsubstrate inhibitor of high-affinity glutamate uptake. *Br. J. Pharmacol.* **140**(5):839-846.

Esslinger CS, Cybulski KA and Rhoderick JF (2005) Ngamma-aryl glutamine analogues as probes of the ASCT2 neutral amino acid transporter binding site. *Bioorg. Med. Chem.* **13**(4):1111-1118.

MOL #75648

Eswar N, Webb B, Marti-Renom MA, Madhusudhan MS, Eramian D, Shen MY, Pieper U and Sali A (2007) Comparative protein structure modeling using MODELLER. *Curr. Protoc. Protein Sci.* **Chapter 2**:Unit 2 9.

Fuchs BC and Bode BP (2005) Amino acid transporters ASCT2 and LAT1 in cancer: partners in crime? *Semin. Cancer Biol.* **15**(4):254-266.

Gliddon CM, Shao Z, LeMaistre JL and Anderson CM (2009) Cellular distribution of the neutral amino acid transporter subtype ASCT2 in mouse brain. *J. Neurochem.* **108**(2):372-383.

Greenfield A, Grosanu C, Dunlop J, McIlvain B, Carrick T, Jow B, Lu Q, Kowal D, Williams J and Butera J (2005) Synthesis and bi ological activities of aryl-ether-, biaryl-, and fluorene-aspartic acid and diaminopropionic acid analogs as potent inhibitors of the high-affinity glutamate transporter EAAT-2. *Bioorg. Med. Chem. Lett.* **15**(22):4985-4988.

Grewer C, Balani P, Weidenfeller C, Bartusel T, Tao Z and Rauen T (2005) Individual subunits of the glutamate transporter EAAC1 homotrimer function independently of each other. *Biochemistry* **44**(35):11913-11923.

Grewer C and Grabsch E (2004) New inhibitors for th e neutral amino acid transporter ASCT2 reveal its Na+-dependent anion leak. *J. Physiol.* **557**(Pt 3):747-759.

Grewer C, Watzke N, Wiessner M and Rauen T (2000) Glutamate translocation of the neuronal glutamate transporter EAAC1 occurs within milliseconds. *Proc. Natl. Acad. Sci. U S A* **97**(17):9706-9711.

Hamill OP, Marty A, Neher E, Sakmann B and Sigworth FJ (1981) Improved patch-clamp techniques for h igh-resolution current recording from c ells and cell-free membrane patches. *Pflugers Arch.* **391**(2):85-100.

Huang Z and Tajkhorshid E (2008) Dynamics of the extracellular gate and ion-substrate coupling

in the glutamate transporter. *Biophys. J.* **95**(5):2292-2300.

Luethi E, Nguyen KT, Burzle M, Blum LC, Suzuki Y, Hediger M and Reymond JL (2010) Identification of selective norbornane-type aspartate analogue inhibitors of the glutamate transporter 1 (GLT-1) from the chemical universe generated database (GDB). *J. Med. Chem.* **53**(19):7236-7250.

Neu J, Shenoy V and Chakrabarti R (1996) Glutamine nutrition and metabolism: where do we go from here ? *FASEB J.* **10**(8):829-837.

Segawa H, Fukasawa Y, Miyamoto K, Takeda E, Endou H and Kanai Y (1999) Identification and functional characterization of a Na+-independent neutral amino acid transporter with broad substrate selectivity. *J. Biol. Chem.* **274**(28):19745-19751.

Sheehan JC, Goodman M and Hess GP (1956) Peptide Derivatives Containing Hydroxyamino Acids. *J. Am. Chem. Soc.* **78**(7):1367-1369.

Shimamoto K, Lebrun B, Yasuda-Kamatani Y, Sakaitani M, Shigeri Y, Yumoto N and Nakajima T (1998) DL-threo-beta -Benzyloxyaspartate, A Potent Blocker of Excitatory Amino Acid Transporters. *Mol. Pharmacol.* **53**(2):195-201.

Soding J, Biegert A and Lupas AN (2005) The HHpred interactive server for protein homology detection and structure prediction. *Nucleic Acids Res.* **33**(Web Server issue):W244-248.

Trott O and Olson AJ (2010) AutoDock Vina: improving the speed and accuracy of docking with a new scoring function, efficient optimization, and multithreading. *J. Comput. Chem.* **31**(2):455-461.

Utsunomiya-Tate N, Endou H and Kanai Y (1996) Cloning and Functional Characterization of a System ASC-like Na+-dependent Neutral Amino Acid Transporter. *J. Biol. Chem.* **271**(25):14883-14890.

Wallner B and E lofsson A (2003) Can correct protein models be identified? *Protein Sci.* **12**(5):1073-1086.

Watzke N, Bamberg E a nd Grewer C (2001) Early intermediates in the transport cycle of the neuronal excitatory amino acid carrier EAAC1. *J. Gen. Physiol.* **117**(6):547-562.

Watzke N and Grewer C (2001) The anion conductance of the glutamate transporter EAAC1 depends on the direction of glutamate transport. *FEBS Lett.* **503**(2-3):121-125.

Wolf LK (2009) New software and Websites for th e Chemical Enterprise. *Chemical & Engineering News* **87**:31.

Yernool D, Boudker O, Jin Y and Gouaux E (2004) Structure of a g lutamate transporter homologue from Pyrococcus horikoshii. *Nature* **431**(7010):811-818.

Zerangue N and Kavanaugh MP (1996) ASCT-1 Is a N eutral Amino Acid Exchanger with Chloride Channel Activity. *J. Biol. Chem.* **271**(45):27991-27994.

Footnotes

Current address of Taniya Thomas: 4 Brighton Lane, New City, NY 10956.

Figure legends

Figure 1: (A) Superposition of the native aspartate ligand from the GltPh 2NWL structure (pink ligand) with the L-Asp complex predicted by Autodock Vina (based on 2NWX, green ligand). **(B)** Superposition of the L-Ser (green) and L-Asn (yellow) ligands docked to the ASCT2(2NWX) homology model (grey structure). The GltPh2NWX structure with the bound ligand, Asp (pink), is shown in turquois. The amino acid side chains in a distance of 4 Å from the ligands are highlighted as lines.

Figure 2: Summary of structures of amino acid substrates and inhibitors used in this study, and a summary of the synthetic procedures.

Figure 3: (A) Superposition of the native TBOA ligand from the GltPh 2NWW structure (turquois ligand) with the L-Bzl-Ser complex (pose 5) predicted by Autodock Vina (based on 2NWW homology model, grey ligand). **(B)** Surface representation of the predicted inhibitor binding site.

Figure 4: (A) Original traces of inward anion currents elicited by the application of full and partial substrates to ASCT2 at the timing and concentration indicted by the grey bar. The baseline current was subtracted. The membrane potential was 0 mV and the intracellular solution contained 10 mM alanine and 135 mM NaSCN. The extracellular solution contained 140 mM NaMes. **(B)** Dose response curves for two of the substrates (**4c**, isopropyl-, squares, and **6c**, ethyl-, circles). The solid lines represent fits according to the Michaelis Menten equation.

Figure 5: (A) Original traces of inward anion currents elicited by the application of alanine (left trace) and inhibited leak anion current by the application of inhibitors to ASCT2 at the timing

and concentration indicted by the grey bar. The baseline current was subtracted. The membrane

potential was 0 mV and the intracellular solution contained 10 mM alanine and 135 mM NaSCN.

The extracellular solution contained 140 mM NaMes. **(B)** Dose response curves for two of the

inhibitors (**2c** and **3c**). The solid lines represent fits according to the Michaelis Menten equation.

(C) 3c inhibits the current response to 200 μM alanine (ionic conditions as in (A)). **(D)** Inhibition

constant, K_I, for serine biphenyl-4-carboxylate (**5c**) at different concentrations of alanine. The

dashed lines show the relationship expected for competitive inhibition, according to equation (1).

The fact that two lines are shown reflects the error in the K_m determined for alanine.

$$K_I(S) = K_I(0) + [S]\frac{K_I(0)}{K_m(\text{alanine})} \tag{1}$$

In this equation, [S] is the concentration of the substrate (alanine), and $K_I(0)$ is the inhibition

constant for serine biphenyl-4-carboxylate in the absence of alanine. **(E)** For inhibition of the

currents in the presence of both inhibitor (**5c**) and alanine (shown here for 200 μM alanine) the

following equation was used to fit the data:

$$\frac{I_{inh+ala}}{I_{max}} = \left(\frac{I_{max} - I_{ala}}{I_{max}}\right)\frac{[I]}{[I] + K_I} + \frac{I_{ala}}{I_{max}} \tag{2}$$

In this equation I_{max} represents the current for inhibitor alone, in the absence of alanine, and K_I is

the inhibition constant for the inhibitor in the presence of alanine (in this case 200μM).

Figure 6: Inhibitor dissociation kinetics. **(A)** Rapid solution exchange from a solution containing

only extracellular buffer (control, black dots) to a solution containing buffer + 2 mM alanine, as

indicated by the bars (top). The red dots shows an analogous experiment, in which the cell was

pre-incubated with 1 mM 3c. Subsequent application of alanine leads to the displacement of 3c,

allowing the determination of dissociation kinetics. The baseline current was subtracted. The

membrane potential was 0 mV and the intracellular solution contained 10 mM alanine and 135

mM NaSCN. The extracellular solution contained 140 mM NaMes. **(B)** Quantification of time constants from the exponential fits shown as solid lines in (A). Note that the time constant for the alanine activation of the current is limited by the time constant of the solution exchange.

Figure 7: Structure-activity relationships of ASCT2 ligands. Dependence of the apparent dissociation constant $(\log(1/K))$ on the volume of the side chain substituent **(A)** and the log(P) of the substituent **(B)**. The substituent was defined as all side chain atoms, starting from C_β, and excluding C_α and the α carboxy and amino groups. Substrates are shown as open symbols and inhibitors are filled symbols.

Figure 8: Predicting substrate, partial substrate, or inhibitor behavior: The direction of the anion current scales with the side chain volume. The anion current response was calculated relative to that induced by saturating alanine concentration (all at 0 mV).

	ASCT2 Homology model based on 2NWX			ASCT2 Homology model based on 2NWW			
	No. of evaluated poses	No. of poses with native α-NH$_2$, COOH	ΔG (kcal/mol)	No. of evaluated poses	No. of poses with native α-NH$_2$, COOH	ΔG (kcal/mol)	ΔG(2NWX)/ ΔG(2NWW)
Serine	9	1	-4.3 (pose 4)	5	2	-3.7 (pose 1)	1.16
Asparagine	9	1	-4.5 (pose 8)	5	2	-4.1 (pose 3)	1.10
Glutamine	9	1	-5.4 (pose 2)	5	2	-4.4 (pose 3)	1.23
-Ethyl (6c)	5	1	-5.8 (pose 0)	5	4	-4.7 (pose 0)	1.23
-Isopropyl (4c)	5	1	-5.7 (pose 2)	8	2	-4.3 (pose 5)	1.33
-Cyclohexyl (1c)	9	1	-3.8 (pose 0)	9	4	-5.3 (pose 1)	0.72
-Bzl-Ser	9	2	-4.6 (pose 0)	7	4	-5.2 (pose 1)	0.88
-Naphtyl (3c)	5	0	-	7	3	-6.1 (pose 5)	-
-Biphenyl (5c)	9	0	-	9	2	-6.6 (pose 6)	-
-Fluorenyl (2c)	6	0	-	8	2	-6.4 (pose 5)	-
	Aspartate transporter 2NWX			Aspartate transporter 2NWW			
Aspartate	5	1	-5.5 (pose 0)	5	1	-4.3 (pose 2)	1.28

Table 1: Parameters for ASCT2 substrates and inhibitors obtained by docking using Autodock Vina.

	K_m (µM)	Relative current
L-Alanine	40 ± 6	1.00
L-Glutamine	25 ± 1	0.98 ± 0.04
-Ethyl (6c)	280 ± 30	1.1 ± 0.06
-Isopropyl (4c)	4700 ± 500	0.26 ± 0.1
-Cyclohexyl (1c)	N.D.	0
-Bzl-Ser	900 ± 400	-0.27 ± 0.1
-Naphtyl (3c)	107 ± 29	-0.22 ± 0.03
-Biphenyl (5c)	30 ± 6	**-0.43 ± 0.07**
-Fluorenyl (2c)	40 ± 12	-0.29 ± 0.04

Table 2: Kinetic properties of ASCT2 substrates and inhibitors. All values are listed for $V_m = 0$ mV. Currents are listed relative to the anion current induced by saturating [alanine].
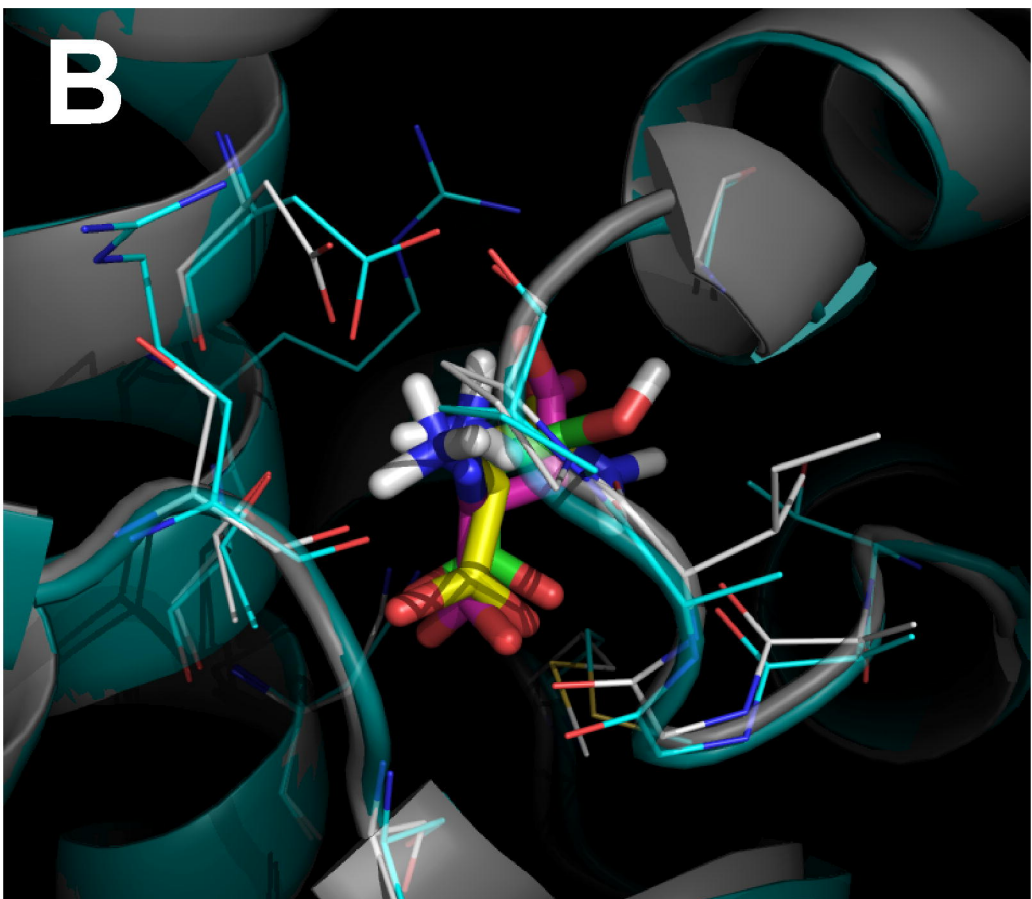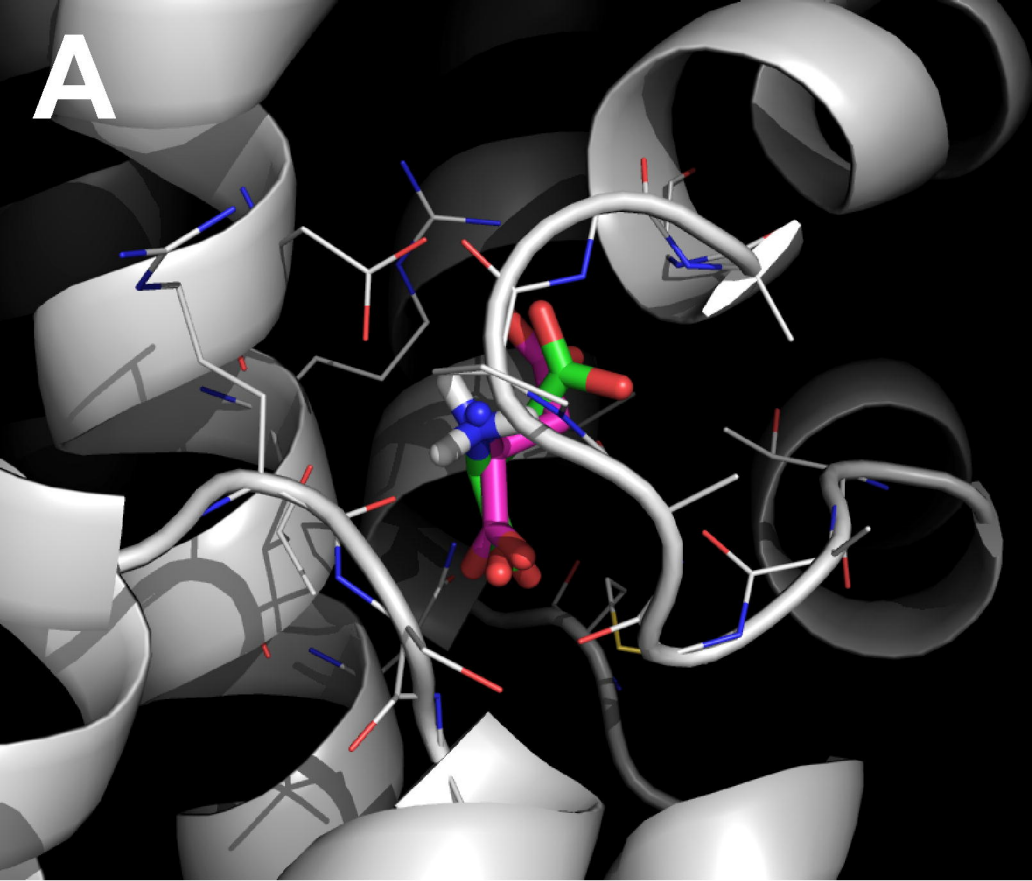
Figure 1
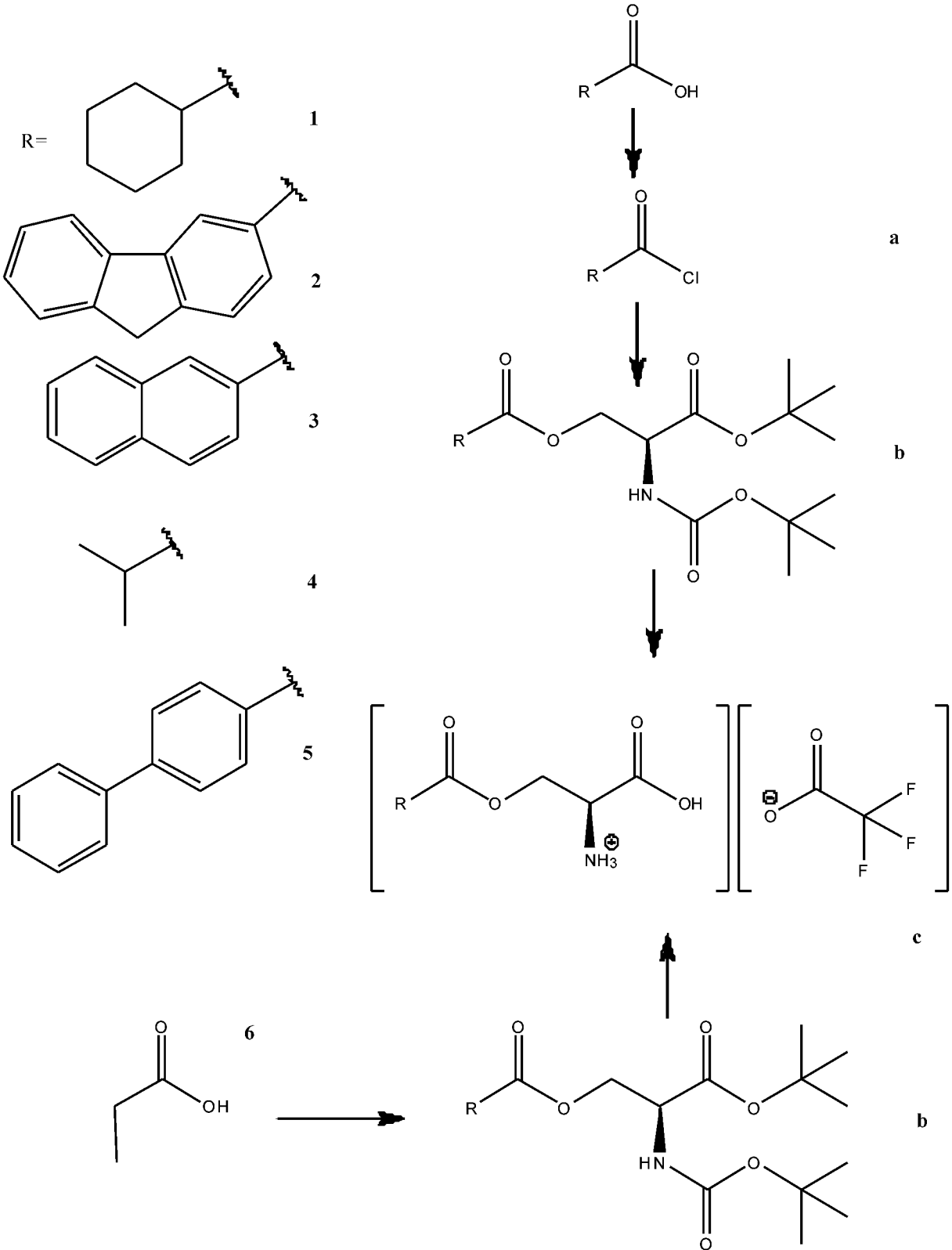
Figure 2
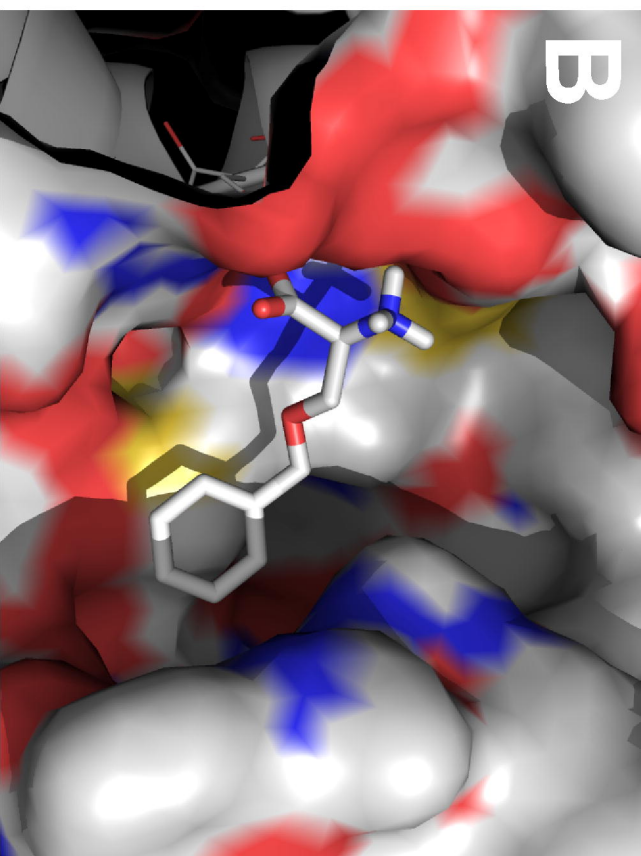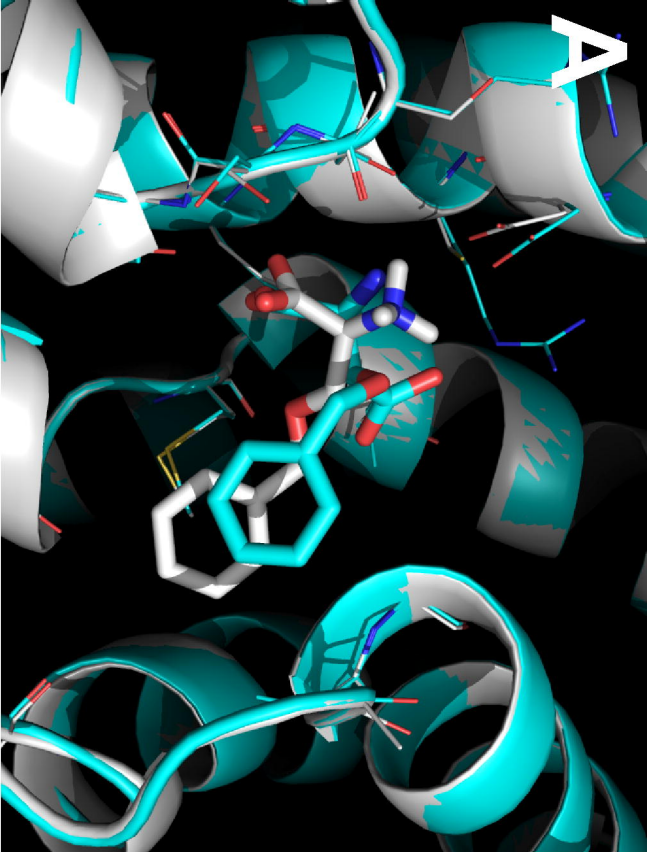
Figure 3
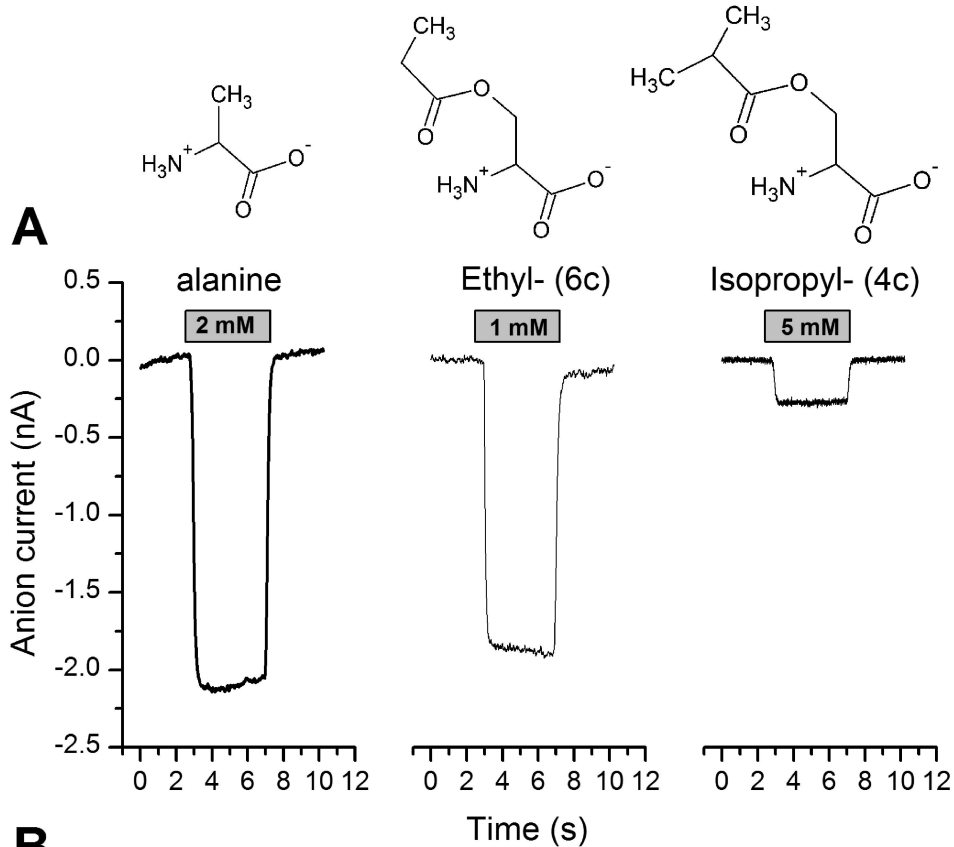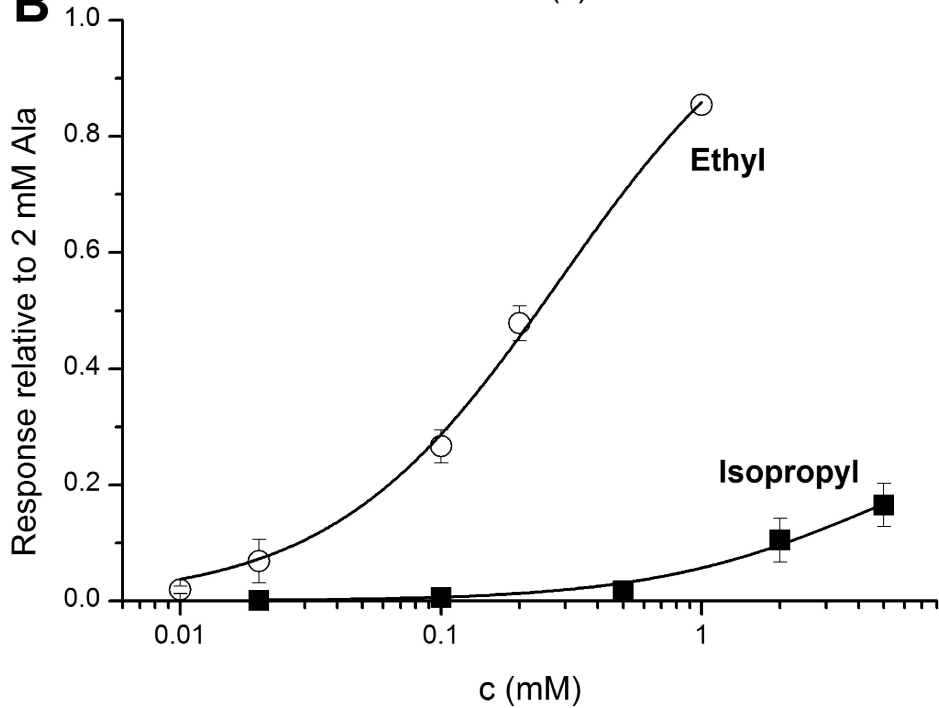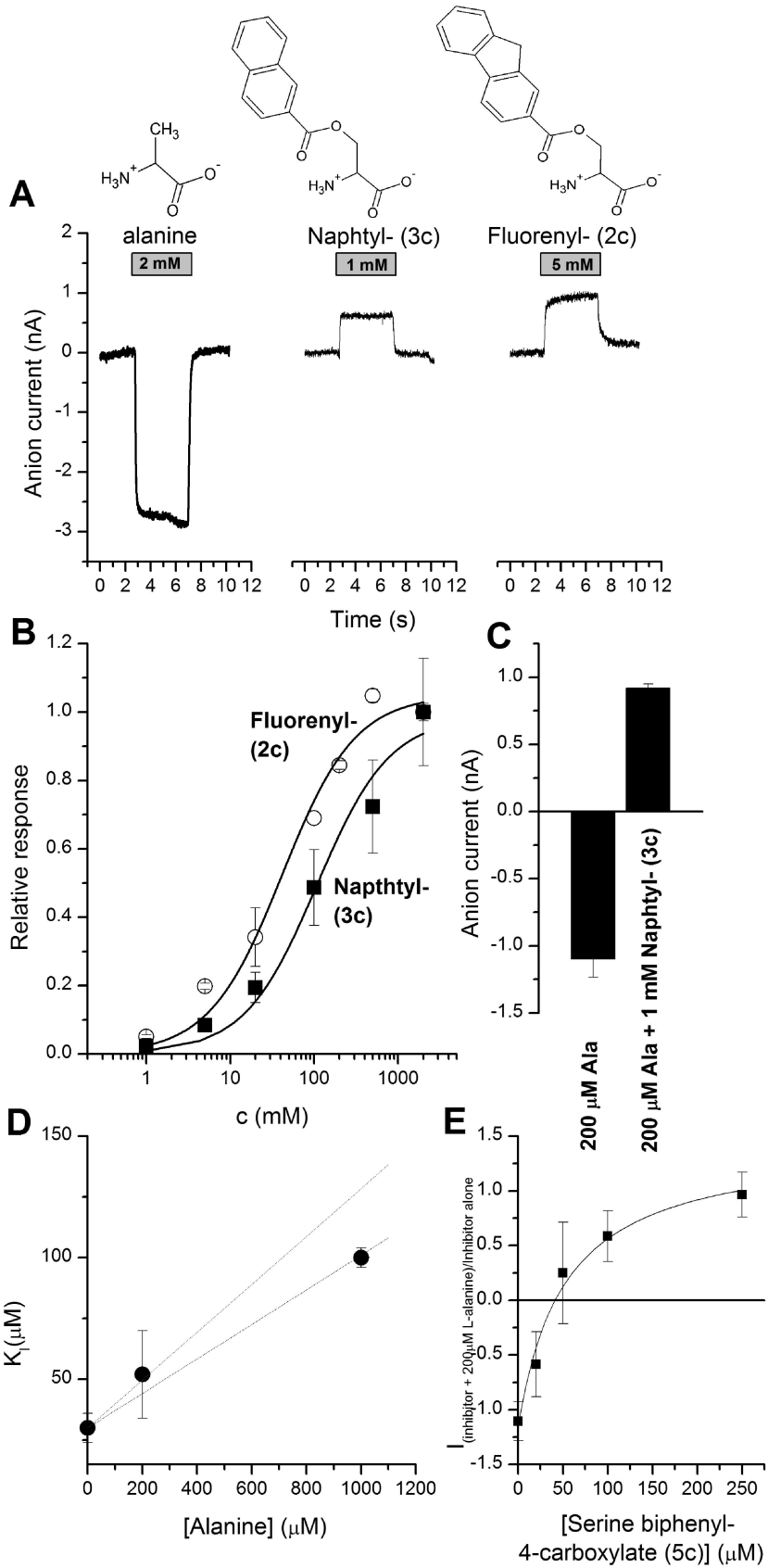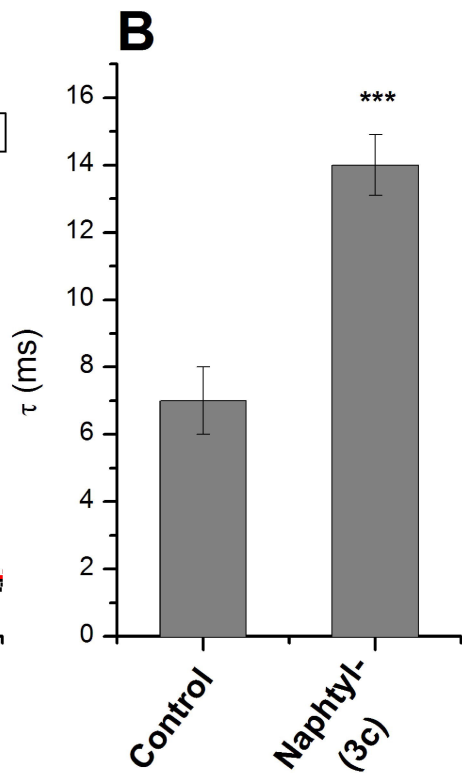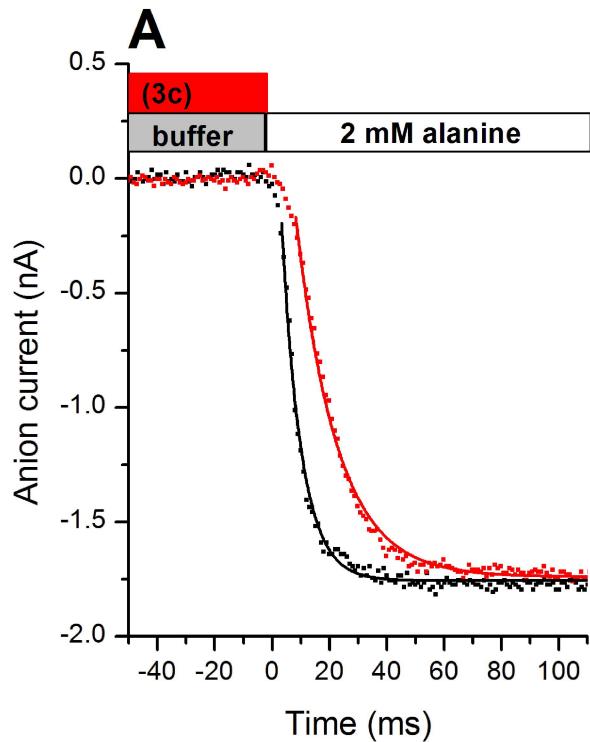
Figure 4

Figure 5

Figure 6

Figure 7

Figure 8